



# Sensory feedback restoration in leg amputees improves walking speed, metabolic cost and phantom pain

## Journal Article

### Author(s):

Petrini, Francesco M.; Bumbasirevic, Marko; [Valle, Giacomo](#) ; Ilic, Vladimir; Mijović, Pavle; Čvančara, Paul; Barberi, Federica; Katic, Natalija; Bortolotti, Dario; Andreu, David; Lechler, Knut; Lesic, Aleksandar; Mazic, Sanja; Mijović, Bogdan; Guiraud, David; Stieglitz, Thomas; Alexandersson, Asgeir; Micera, Silvestro; [Raspopovic, Stanisa](#) 

### Publication date:

2019-09

### Permanent link:

<https://doi.org/10.3929/ethz-b-000386604>

### Rights / license:

[In Copyright - Non-Commercial Use Permitted](#)

### Originally published in:

Nature Medicine 25(9), <https://doi.org/10.1038/s41591-019-0567-3>

### Funding acknowledgement:

759998 - Restoring natural feelings from missing or damaged peripheral nervous system by model-driven neuroprosthesis (EC)

# Sensory feedback restoration in leg amputees improves walking speed, metabolic cost and phantom pain

Francesco Maria Petrini<sup>1,2,3,16</sup>, Marko Bumbasirevic<sup>4,5,16</sup>, Giacomo Valle<sup>6</sup>, Vladimir Ilic<sup>7</sup>, Pavle Mijović<sup>8</sup>, Paul Čvančara<sup>9</sup>, Federica Barberi<sup>2,3,6</sup>, Natalija Katic<sup>10</sup>, Dario Bortolotti<sup>2</sup>, David Andreu<sup>11</sup>, Knut Lechler<sup>12</sup>, Aleksandar Lesic<sup>4,5</sup>, Sanja Mazic<sup>13</sup>, Bogdan Mijović<sup>8</sup>, David Guiraud<sup>11</sup>, Thomas Stieglitz<sup>14</sup>, Asgeir Alexandersson<sup>12</sup>, Silvestro Micera<sup>3,6,17</sup> and Stanisa Raspopovic<sup>1,2,17\*</sup>

Conventional leg prostheses do not convey sensory information about motion or interaction with the ground to above-knee amputees, thereby reducing confidence and walking speed in the users that is associated with high mental and physical fatigue<sup>1–4</sup>. The lack of physiological feedback from the remaining extremity to the brain also contributes to the generation of phantom limb pain from the missing leg<sup>5,6</sup>. To determine whether neural sensory feedback restoration addresses these issues, we conducted a study with two transfemoral amputees, implanted with four intraneural stimulation electrodes<sup>7</sup> in the remaining tibial nerve (ClinicalTrials.gov identifier NCT03350061). Participants were evaluated while using a neuroprosthetic device consisting of a prosthetic leg equipped with foot and knee sensors. These sensors drive neural stimulation, which elicits sensations of knee motion and the sole of the foot touching the ground. We found that walking speed and self-reported confidence increased while mental and physical fatigue decreased for both participants during neural sensory feedback compared to the no stimulation trials. Furthermore, participants exhibited reduced phantom limb pain with neural sensory feedback. The results from these proof-of-concept cases provide the rationale for larger population studies investigating the clinical utility of neuroprostheses that restore sensory feedback.

Despite advances in the development of lower-limb prosthetics<sup>8</sup>, the potential benefits of restoring sensory feedback from such devices to transfemoral (above-knee) or transtibial (below-knee) amputees has not been investigated. Most surgery techniques<sup>9</sup> and noninvasive methods<sup>10–12</sup> to restore sensory feedback have been tested only in transtibial amputations, which produce a less disabling clinical condition than transfemoral amputation<sup>1,3</sup>. Direct neural stimulation through transversal intrafascicular multichannel electrodes (TIMES)<sup>7</sup> has enabled upper-limb amputees to feel touch sensations from the missing hand and to exploit them for long-term prosthesis control<sup>13,14</sup>. Only

a few trials<sup>15,16</sup> with direct nerve stimulation that did not show clear benefits for the leg amputees have been conducted. Restoring sensory feedback from the phantom hand of upper-limb amputees through neural stimulation has been shown to decrease phantom limb pain (PLP)<sup>13,17,18</sup>. However, the efficacy of low-frequency nerve stimulation<sup>19</sup> has never been investigated for treating PLP in leg amputees.

In this study, we recruited two volunteers with transfemoral amputation as a consequence of traumatic events (Supplementary Table 1). These volunteers were implanted with four TIMES<sup>7</sup> in the nearest portion of the residual tibial nerve to the amputation for more than 90 d each (top right in Fig. 1 and Extended Data Fig. 1).

We characterized the responses of the volunteers to nerve stimulation during the first month of the study. Short pulse trains of electrical current varying in intensity, duration and frequency were injected into each active site. The volunteers described the sensation in terms of type, location, extent and intensity. Physiologically plausible sensations, that is, reported by the volunteers similarly to the ones perceived with the nonamputated leg, of touch, pressure, vibration and muscle activation were elicited over the phantom foot sole and lower leg (Extended Data Fig. 2a–c). Other less physiologically plausible percepts such as tingling, pulsation and electricity were evoked, similarly to previous reports with the same technology<sup>13</sup>, which were not used for the neuroprosthesis and pain tests. The extent of the sensations was localized and did not change (or changed only slightly) when the injected charge in the tibial nerve was varied (Extended Data Fig. 2d). The intensity of the perceived sensations was proportional to the injected charge (Extended Data Fig. 2e). We used the map of sensations to calibrate the neuroprosthesis (Fig. 1), which consisted of the intraneural electrodes, a stimulator, an external controller and a sensorized insole, located under a custom-made transfemoral prosthesis (composed

<sup>1</sup>Department of Health Sciences and Technology, Institute of Robotics and Intelligent Systems, Swiss Federal Institute of Technology Zürich, Zürich, Switzerland. <sup>2</sup>SensArs Neuroprosthetics, Lausanne, Switzerland. <sup>3</sup>Bertarelli Foundation Chair in Translational Neuroengineering, Centre for Neuroprosthetics and Institute of Bioengineering, School of Engineering, École Polytechnique Fédérale de Lausanne, Lausanne, Switzerland. <sup>4</sup>Orthopaedic Surgery Department, School of Medicine University of Belgrade, Belgrade, Serbia. <sup>5</sup>Clinic of Orthopaedic Surgery and Traumatology, Clinical Centre of Serbia, Belgrade, Serbia. <sup>6</sup>The BioRobotics Institute, Sant'Anna School of Advanced Studies, Pisa, Italy. <sup>7</sup>Faculty of Sport and Physical Education, School of Medicine, University of Belgrade, Belgrade, Serbia. <sup>8</sup>mBrainTrain d.o.o., Belgrade, Serbia. <sup>9</sup>Laboratory for Biomedical Microtechnology, Department of Microsystems Engineering, University of Freiburg, Freiburg, Germany. <sup>10</sup>Institute Mihajlo Pupin, Belgrade, Serbia. <sup>11</sup>Inria, University of Montpellier, Montpellier, France. <sup>12</sup>Össur, Reykjavik, Iceland. <sup>13</sup>Institute of Medical Physiology, School of Medicine, University of Belgrade, Belgrade, Serbia. <sup>14</sup>Cluster of Excellence BrainLinks-BrainTools, University of Freiburg, Freiburg, Germany. <sup>15</sup>Bernstein Center Freiburg, University of Freiburg, Freiburg, Germany. <sup>16</sup>These authors contributed equally: Francesco Maria Petrini, Marko Bumbasirevic, Giacomo Valle. <sup>17</sup>These authors jointly supervised this work: Silvestro Micera,

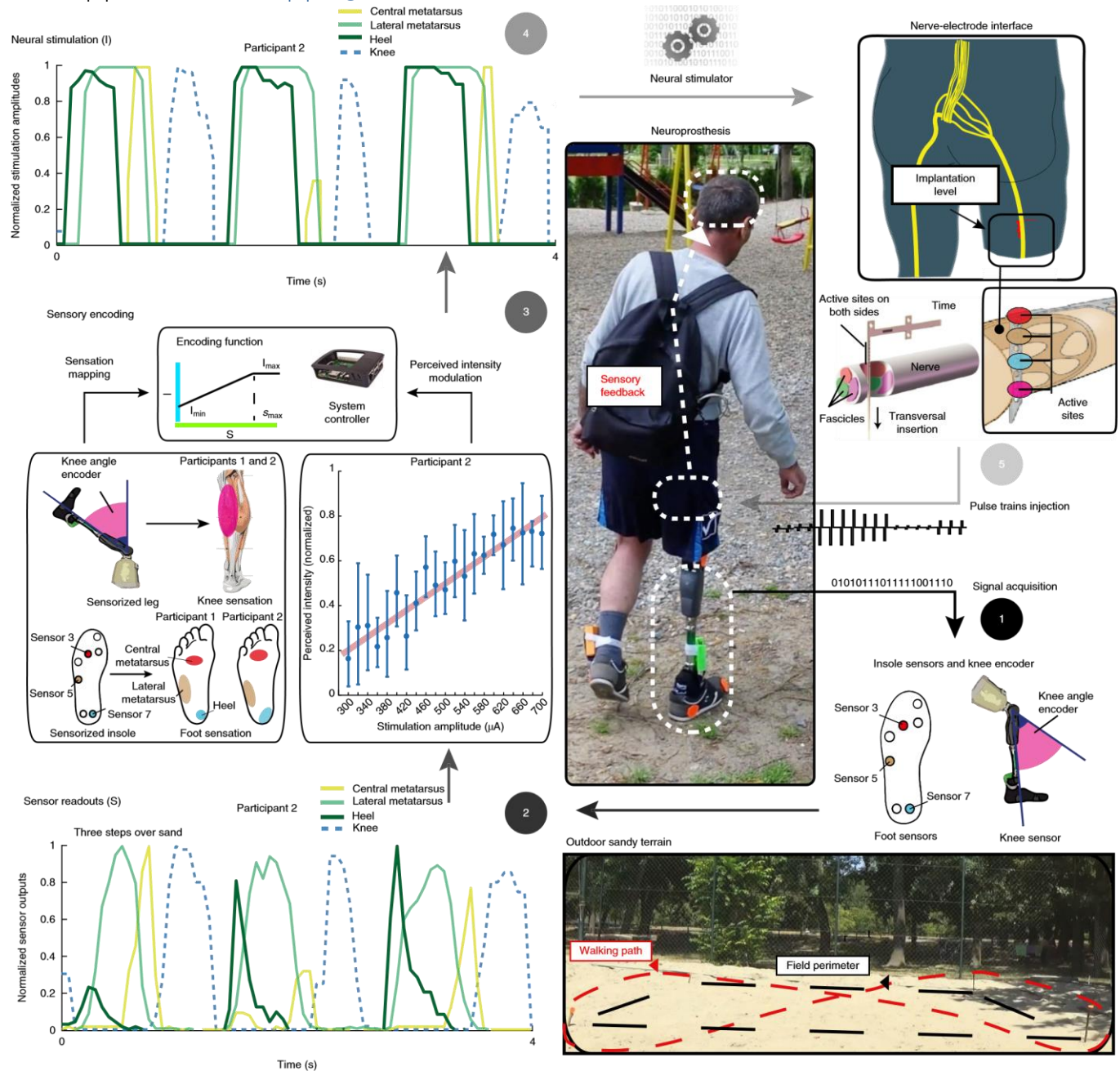


**Fig. 1 | Neuroprosthesis.** Participant wearing the whole system composed of a sensorized insole placed under the foot (1), with the electronics fastened to the ankle, a custom-made lower-limb prosthesis (composed of commercially available prosthetic components) in which the microprocessor-controlled knee has an integrated knee encoder (1), an external controller and an external stimulator. The participant walks over an outdoor terrain making a figure of eight. Data from both insoles (participants wore a sensorized insole also on the healthy leg in every task) and the knee encoder are transmitted in realtime via Bluetooth to the external controller (2). The acquired signals are converted into neural stimulation by means of an encoding algorithm according to sensation mapping and perceived intensity modulation (3). The resulting neural stimulation (4) is injected through the neural implants (5) evoking somatotopic and homologous sensations in the phantom foot and leg during walking in real time.

of commercially available prosthetic components: RHEO KNEE XC, PRO-FLEX XC foot and transfemoral flexible brim socket fitted to an Icross Seal-In X5 TF silicon liner, Ossur hf, Iceland). The microprocessor-controlled knee has an integrated knee encoder. The readouts of three of the insole pressure sensors and the knee encoder were used as control inputs for the intraneural stimulation of four active sites (Fig. 1). Three active sites elicited a sensation of touch, pressure or vibration in the central metatarsus, lateral metatarsus and heel, and one active site elicited a sensation

of activation of the phantom calf (interpreted as knee flexion), for each participant (Fig. 1). The perceptions of foot contact and knee motion elicited through direct nerve stimulation were integrated, without prior training, by the users while walking with the prosthesis (Supplementary Video 1). To verify whether the use of the neuroprosthesis could provide participants with clinical benefits, we challenged them with walking tasks. Trials with sensory feedback were compared against those without sensory feedback (no feedback).

The speed and confidence of participants were assessed while they walked outdoors over a path traced in the sand (Fig. 1 and Supplementary Video 2). Confidence in the prosthesis was assessed by participants using a number from 0 to 10. In the test sessions, participants' speeds were significantly higher when sensory feedback was provided (Fig. 2a). During the last session, participant 1 walked at a higher speed with an improvement of  $3.56 \pm 1.45 \text{ m min}^{-1}$  (mean  $\pm$  s.d.,  $P < 0.05$ ), while participant 2 showed an improvement of  $5.68 \pm 0.44 \text{ m min}^{-1}$  (mean  $\pm$  s.d.,  $P < 0.05$ ). The reported confidence level (Fig. 2b) improved from  $4.85 \pm 0.69$  to  $7.71 \pm 0.48$  (mean  $\pm$  s.d.,  $P < 0.05$ ) for participant 1, and from  $2.7 \pm 1.09$  to  $5.55 \pm 0.8$  (mean  $\pm$  s.d.,  $P < 0.05$ ), for participant 2. To assess the amount of mental effort expended during the use of the prosthesis while walking, participants were involved in a dual-task paradigm, as suggested by Wickens et al.<sup>20</sup> and many follow-up studies (see Methods). Specifically, participants were required to walk (primary task) and silently count target tones that were delivered through headphones (secondary task), while ignoring all nontarget tones<sup>21</sup> (see Methods). Paying attention to the target tones was expected to elicit a distinguishable and higher P300 event-related potential (ERP) component<sup>22,23</sup> amplitude, than the one elicited by the nontarget tones. Higher P300 amplitude would show more mental resources available for the secondary task, indicating that participants did not allocate their attention solely to the primary task (that is, prosthesis use). The  $2 \times 2$  analysis of variance (ANOVA; (sensory feedback versus no feedback  $\times$  target versus nontarget tone) revealed that the P300 amplitude differed depending on the tone for both participants ( $P < 0.05$ , Fig. 2c–e). In addition, we obtained the main effect of the interaction condition  $\times$  tone for both participants ( $P < 0.05$ , Fig. 2c–e). The post hoc analysis revealed that the cortical response for both participants was significantly higher for the target than for the nontarget tones (Fig. 2c–e), for the sensory feedback condition ( $P < 0.01$ ) but not for the no feedback condition ( $P > 0.05$ ). This suggests that in the no feedback walking conditions, participants could not direct attention to the dual task, indicating a higher mental effort than when walking with sensory feedback.

To determine the effect of the neuroprosthesis on physical fatigue, participants were asked to walk outdoors and indoors while their metabolic consumption (that is, the volume of oxygen ( $\text{VO}_2$ )) was measured. Indoors, participants were asked to walk on a treadmill while the speed was increased by  $0.5 \text{ km h}^{-1}$  every minute. Outdoor walking was performed on grass and participants had to ambulate at a self-selected speed. Indoors, both participants reached a  $0.5 \text{ km h}^{-1}$  higher speed on the treadmill when stimulation was provided (Fig. 3a), since they did not feel confident enough to achieve the same speed without sensory feedback. Also, both participants had a lower mean rate of oxygen uptake during the sensory feedback trials: significant differences between two corresponding speeds were found at most speeds ( $P < 0.05$ ; Fig. 3a).

Outdoors, participant 1 had lower  $\text{O}_2$  consumption and maintained walking pace, while participant 2 maintained  $\text{O}_2$  consumption but achieved a faster pace (Supplementary Table 2) when sensory feedback was provided. These results are indicative of an improvement in overall gait efficiency measured as net  $\text{VO}_2$  (Methods):  $0.261 \pm 0.027$  versus  $0.215 \pm 0.026 \text{ ml kg}^{-1} \text{ m}^{-1}$  (mean  $\pm$  s.d.,  $P < 0.01$ ), no feedback and sensory feedback, respectively for participant 1, and  $0.199 \pm 0.024$  versus  $0.175 \pm 0.022 \text{ ml kg}^{-1} \text{ m}^{-1}$  (mean  $\pm$  s.d.,  $P < 0.01$ ) for participant 2 (Fig. 3b).

To verify whether low-frequency neural stimulation<sup>19</sup> was effective in reducing PLP, participants received two types of pain treatment: frequency-invariant and frequency-variant stimulation,

where frequency of stimulation was fixed and variable, respectively. Both frequency-invariant and frequency-variant stimulations target the area of pain through localized and physiologically plausible sensations. Given that frequency-variant emulates the Poisson distribution occurrence of afferent fiber firings<sup>24</sup>, we hypothesized that it would elicit more pleasant and physiologically plausible sensations that would thus be more effective in terms of pain relief<sup>25,26</sup>. Ten-minute trains of stimulation were delivered and controlled with sessions of no stimulation at all. PLP evolution was measured through the Neuropathic Pain Symptom Inventory (NPSI, from 0 to 100)<sup>27</sup> and visual analog scale (VAS, from 0 to 40)<sup>28</sup> questionnaires, which were provided before and after the 10-min stimulation sessions. The pain level decreased significantly after the frequency-invariant and frequency-variant 10-min stimulation sessions for participant 1 ( $P < 0.05$ ; Fig. 4a,b and Extended Data Fig. 3a,b) and participant 2 ( $P < 0.05$ ; Fig. 4e,f and Extended Data Fig. 3e,f). Before and after the single control sessions, no difference in pain level was reported and the effect of these sessions was negligible compared to frequency-invariant and frequency-variant stimulation (Fig. 4b,f and Extended Data Fig. 3b,f). A decrease from the first to the last treatment session was recorded through the NPSI (50 versus 0 for participant 1 and 32 versus 12 for participant 2; Fig. 4a,c,e,g) and VAS (20 versus 0 for participant 1 and 18 versus 9 for participant 2; Extended Data Fig. 3a,c,e,g).

Commercial microprocessor-controlled knees improve participants' self-selected walking speed by about 8% compared to mechanically passive devices<sup>29</sup>. In this study, we show that the speed of participants in outdoor tasks while using a microprocessor-controlled knee (RHEO KNEE XC) was improved even more by sensory feedback ( $>10\%$ ). We hypothesize that the participants managed to increment their walking speed, when provided with sensory feedback, by exerting more force with both limbs on the ground (Extended Data Fig. 4). In fact, unilateral lowerlimb amputees produce an increment in walking speed by pushing stronger with both legs on the ground, the healthy extremity being the one with the highest force increment<sup>30</sup>; we observed a similar behavior (Extended Data Fig. 4). Further detailed analyses are necessary to unveil the codes (if present) explaining what microscopic kinematic parameter is directly correlated with sensory feedback and the change in speed. We found that when using the sensory feedback prostheses outdoors, participants reported an increased sense of confidence in the device and experienced a reduced mental effort. We believe these are promising findings, since they may represent a solution to the high abandonment rate in prostheses use, which is possibly connected to a lack of confidence and low comfort<sup>31</sup>. They also suggest that restoration of the physiologically plausible sensory feedback was intuitively integrated by the participants' central nervous system. These electroencephalography (EEG) results are highly significant because they are derived from recordings executed in naturalistic environment (that is, not in the controlled conditions of the laboratory where there are no noises or distractions, and planned movements are less complex).

Traumatic above-knee amputation is associated with an increased cardiovascular morbidity or mortality rate in the long term<sup>32</sup>, with a relative risk of death by cardiac causes 2.2 times greater compared to healthy controls<sup>33</sup>. Improving the economy of walking through a decrease in  $\text{O}_2$  cost decreases the cardiorespiratory loading and could be very important for counteracting these issues.

A study<sup>34</sup> comparing two microprocessor-controlled knees (C-Leg and RHEO KNEE) and a mechanically passive one (Mauch

SNS hydraulic) showed that when using the RHEO KNEE to walk over ground at a self-selected speed, the metabolic rate decreased by 5% compared with the Mauch SNS and by 3% (no statistical relevance) compared with the C-Leg. In this study, we found that

when restoring sensory feedback to participants using RHEO KNEE XC overground, metabolic costs were lowered even further (gait efficiency of 12% and 17.6% for participants

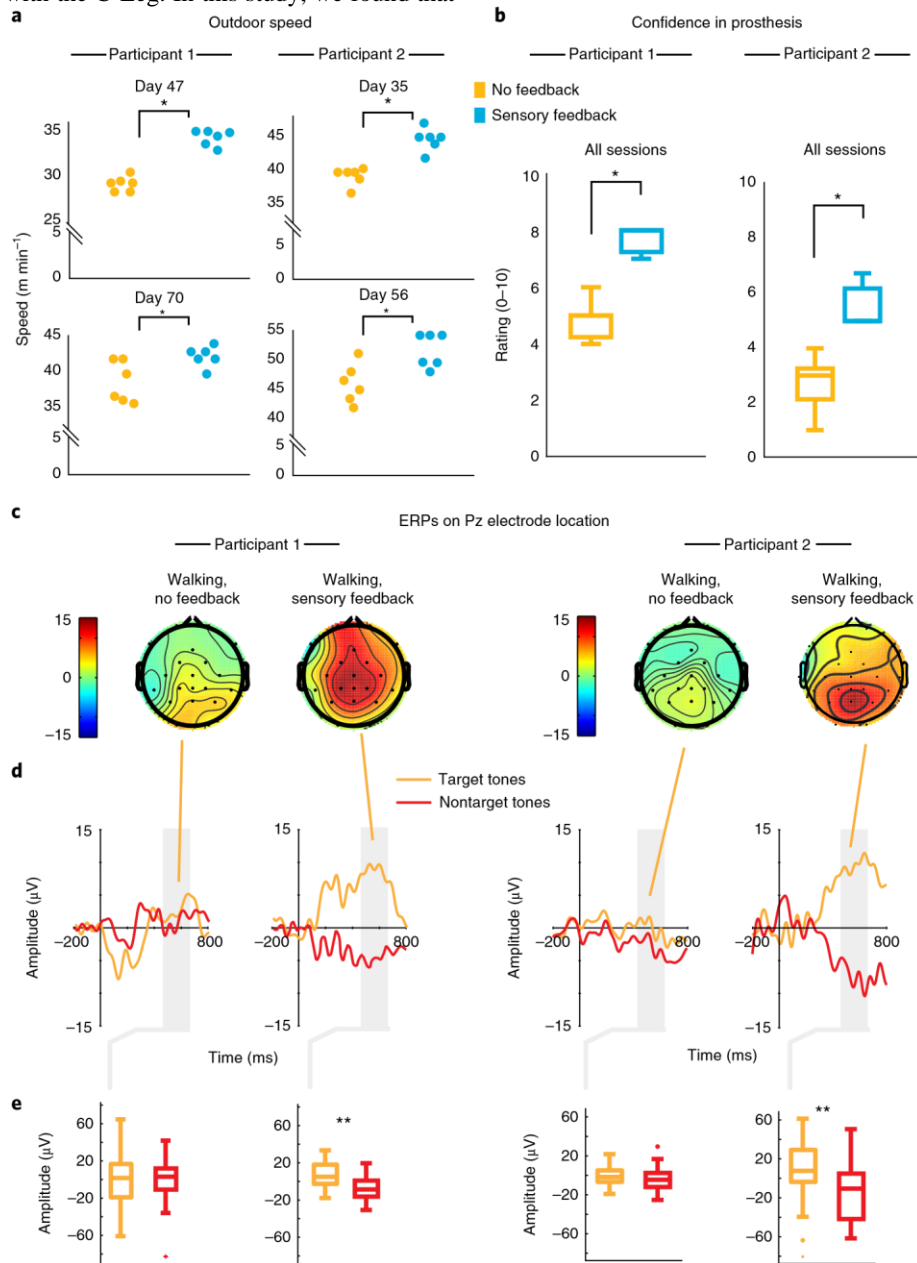


**Fig. 2 | Walking speed, confidence and mental effort assessment.** **a**, Speed when sensory feedback is restored and when it is not during two 6-min outdoor sessions (walking on a sandy terrain) for participants 1 and 2. The dots show the data distribution ( $n = 6$  1-min trials per sensory feedback and no feedback conditions and per session). A Kruskal–Wallis test was performed. For participant 1, the result of the test was  $d.f. = 1$  (between-groups),  $F = 8.4$ ,  $P = 0.0038$  for session 1. The result was  $d.f. = 1$ ,  $F = 4.88$ ,  $P = 0.027$  for session 2. For participant 2, the result was  $d.f. = 1$ ,  $F = 8.5$ ,  $P = 0.0035$  for session 1 and  $d.f. = 1$ ,  $F = 5.49$ ,  $P = 0.019$  for session 2. **b**, Confidence in prosthesis reported by participants after each experimental session ( $n = 12$  reports from 2 sessions of experiments per no feedback and sensory feedback conditions). A Kruskal–Wallis test was performed. For participant 1, the result of the test was  $d.f. = 1$ ,  $F = 80$ ,  $P < 0.00001$ ; for participant 2, it was  $d.f. = 1$ ,  $F = 22.1$ ,  $P = 0.0015$ . **c**, Topographical representation of voltage distribution over the scalp in the P300 window (for the two different participants, a different highest peak latency was obtained) in response to the target tones, for both stimulation conditions. **d**, ERPs elicited during walking with and without sensory feedback and comparison between the target (orange) and nontarget (red) trials. The shaded areas represent the time window for the P300 computation (between 450 and 600 ms after acoustic stimulus presentation). **e**, Distribution of the data in the shaded areas in **(d)**. A  $2 \times 2$  ANOVA (condition: sensory feedback versus no feedback  $\times$  tone target versus nontarget) with post hoc analysis (paired sample  $t$ -test) was performed in **d,e**. The test revealed that the P300 amplitude differed depending on the tone (for participant 1:  $d.f. = 1$ ,  $F = 5.41$ ,  $P = 0.026$ ; for participant 2:  $d.f. = 1$ ,  $F = 10.26$ ,  $P = 0.003$ ). In addition, we obtained the main effect of the interaction condition  $\times$  tone (for participant 1:  $d.f. = 1$ ,  $F = 4.90$ ,  $P = 0.034$ ; for participant 2:  $d.f. = 1$ ,  $F = 5.63$ ,  $P = 0.023$ ). The post hoc analysis revealed that the cortical response for both participants was significantly higher for the target tones than for the nontarget tones, for the sensory feedback participant 1:  $d.f. = 1$ ,  $t = 7.95$ ,  $P < 0.001$ ; for participant 2:

d.f. = 1,  $t = 2.94$ ,  $P = 0.006$ ) but not for the no feedback condition (for participant 1: d.f. = 1,  $t = 0.094$ ,  $P = 0.93$ ; for participant 2: d.f. = 1,  $t = 1.22$ ,  $P = 0.21$ ). For participant 1,  $n = 34$  for each stimulation condition (no feedback and sensory feedback), while for participant 2,  $n = 38$ .  $n$  is the number of included epochs from which the average is calculated. See the Methods for the exact procedure to include the epochs.  $*P < 0.05$ .  $**P < 0.01$ . In each box plot, the thick horizontal line denotes the median, whereas the lower and upper hinges correspond to the first and third quartiles, the whiskers extend from the hinge to the most extreme value no further than  $1.5 \times$  interquartile range from the hinge and the dots beyond the whiskers are outliers.

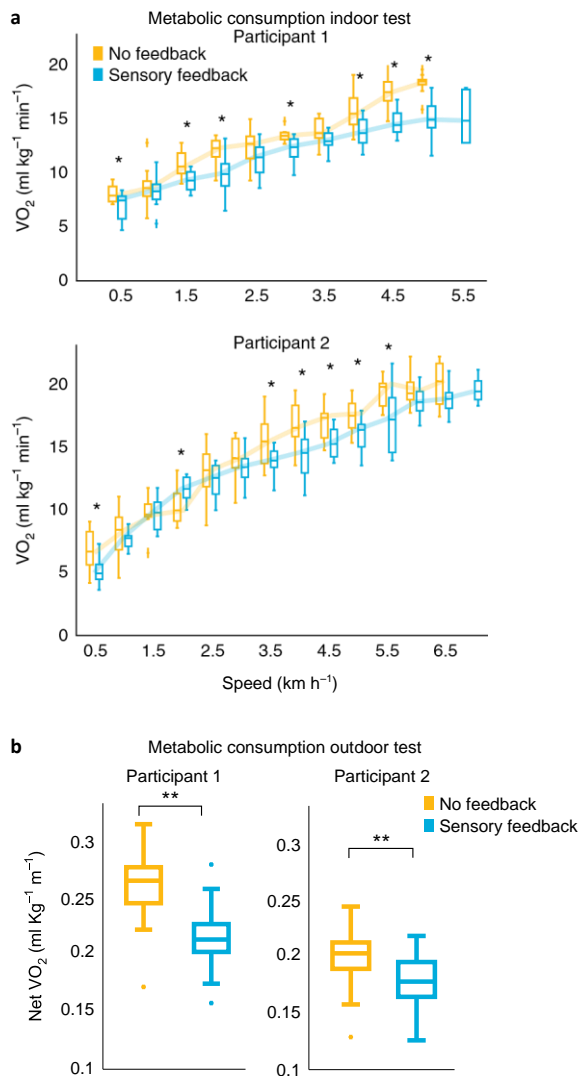


**Fig. 3 | Metabolic consumption assessment.** **a**, Oxygen consumption normalized on individual body mass ( $VO_2$ ) on a treadmill when intraneural stimulation is provided (sensory feedback, light blue) and when it is not (no feedback, orange).  $VO_2$  consumption on the treadmill was recorded in 5-s increments ( $n = 12$  values per minute per stimulation condition) and averaged for each walking speed. **b**, Net  $VO_2$  in the two feedback conditions when participants were walking on the ground. Each  $VO_2$  value is averaged over  $n = 36$  (that is, 3 min of data sampled at 5-s increments per stimulation condition). In each box plot, the thick horizontal line denotes the median, whereas the lower and upper hinges correspond to the first and third quartiles, the whiskers extend from the hinge to the most extreme value no further than  $1.5 \times$  interquartile range from the hinge and the dots beyond the whiskers are outliers. In **a,b**, an ANOVA statistical test was performed. For the indoor task, the  $P$  values for the tested velocities (ascending order) for participant 1 were (0.0131, 0.4296, 0.0009, 0.0023, 0.0776, 0.0036, 0.0682, 0.0072, 0.0001,  $<0.0001$ ), d.f. = 1,  $F = (7.28, 0.65, 14.69, 11.92, 3.43, 10.63, 3.67, 8.76, 23.80, 35.25)$  and for participant

2 (0.0069, 0.27, 0.75, 0.021, 0.29, 0.18, 0.02, 0.004, 0.004, 0.009, 0.007, 0.06, 0.06), d.f. = 1,  $F = (8.89, 1.23, 0.1, 6.18, 1.19, 1.94, 0.07, 10.35, 9.88, 8.02, 8.57, 3.97, 3.96)$ . For participant 1, the result of the tests for the outdoor data was d.f. = 1,  $F = 55.56$ ,  $P < 0.0001$ ; for participant 2, the result was d.f. = 1,  $F = 18.73$ ,  $P < 0.0001$ .  $*P < 0.05$ ,  $**P < 0.01$ .

2 and 1, respectively). Past studies<sup>35</sup> have shown that transfemoral amputees decrease  $VO_2$  by 6.6% when walking with the C-Leg on a treadmill compared to nonmicroprocessor-based prosthetic knees. These studies were performed at a controlled walking speed of about  $3 \text{ km h}^{-1}$ . On the other hand, our treadmill trials clearly indicate that in the majority of acceptable velocities for the participants, restoration of sensory feedback leads to a reduction in mean oxygen uptake rate. Therefore, we found that sensory feedback lowers even further the oxygen consumption of transfemoral amputees using microprocessor-based knees (as it is with the RHEO KNEE XC). We hypothesize that the decrease of metabolic costs when sensory feedback is provided is due to restored symmetry of walking between the two legs (Extended Data Fig. 4) and an incremented self-selected walking speed (Fig. 2 and Supplementary Table 2). Indeed, by walking more symmetrically, participants walk more similarly to healthy counterparts. Healthy walking has a reduced energy consumption compared to amputee walking<sup>36</sup>. Also, since there is an increment in the self-selected walking speed (Fig. 2 and Supplementary Table 2), the metabolic costs decrease. In fact, Detrembleur et al.<sup>37</sup> have shown that there is an inverse correlation between walking energy and self-selected speed in amputees: the smaller the speed, the higher the metabolic consumption since the efficiency of the pendulum-like mechanism is decreased. Interestingly, the results were achieved with two proficient prosthetic users, for whom one might expect limited room for improvement to exist in prosthesis use. Thus, we hypothesize that such a system could be even more useful with participants with a lower walking ability or during rehabilitation.

A 30% reduction in pain on the numeric rating scale (between 0 and 10) has been suggested as a clinically significant outcome<sup>38</sup>. The improvements found in this study were  $>80\%$ , and significant pain suppression was achieved before the electrodes were explanted. The acute (that is, transient) reduction of pain (after every session of stimulation) could be explained by the gate theory (that is, the inhibition exerted by large afferents on the nociceptive spinothalamic pathways<sup>39</sup>). The gradual reduction of pain until complete disappearance, may be due to sensory feedback, which triggered beneficial neuroplastic changes in the brain<sup>5,6</sup>. Since participant 1 did not report any pain after the first month of this pilot study, and participant 2 reported it only sporadically, we could not investigate the impact of the use of the prosthesis on pain levels. We believe this will be interesting for a future study. Frequency-variant stimulation did not produce better results than frequency-invariant stimulation in relieving pain, hence there is no indication of whether one should be used rather than the other. In other words, these results suggest that the paradigm of stimulation does not impact the outcome of pain therapy. However, in this study only two paradigms of stimulation were compared (both

eliciting physiologically plausible localized sensations). Further investigations with more paradigms of stimulation should be conducted to determine the parameter of neural stimulation that impacts pain reduction.

This work presents a proof-of-concept trial aimed at providing preliminary evidence of the benefits that sensory feedback restored through intraneural stimulation gives to leg amputees.

More investigations and tests are necessary to prove whether a more proximal implant (higher amputation level) could provide similar stimulation selectivity. The use of cadaveric trials, computational modeling and computer simulations could help

optimize this technology and the surgical procedure for different amputation levels<sup>40</sup>. An investigation longer than 3 months, with a larger cohort of participants, and with in-home assessments, should be executed to provide more robust data to draw clinically significant conclusions about an improvement in the health and quality of life of patients. Fully implantable devices (without transcutaneous cables) need to be developed to allow such investigation. Overall, this work paves the way for the development of a clinical tool that will significantly improve amputees' health and quality of life.

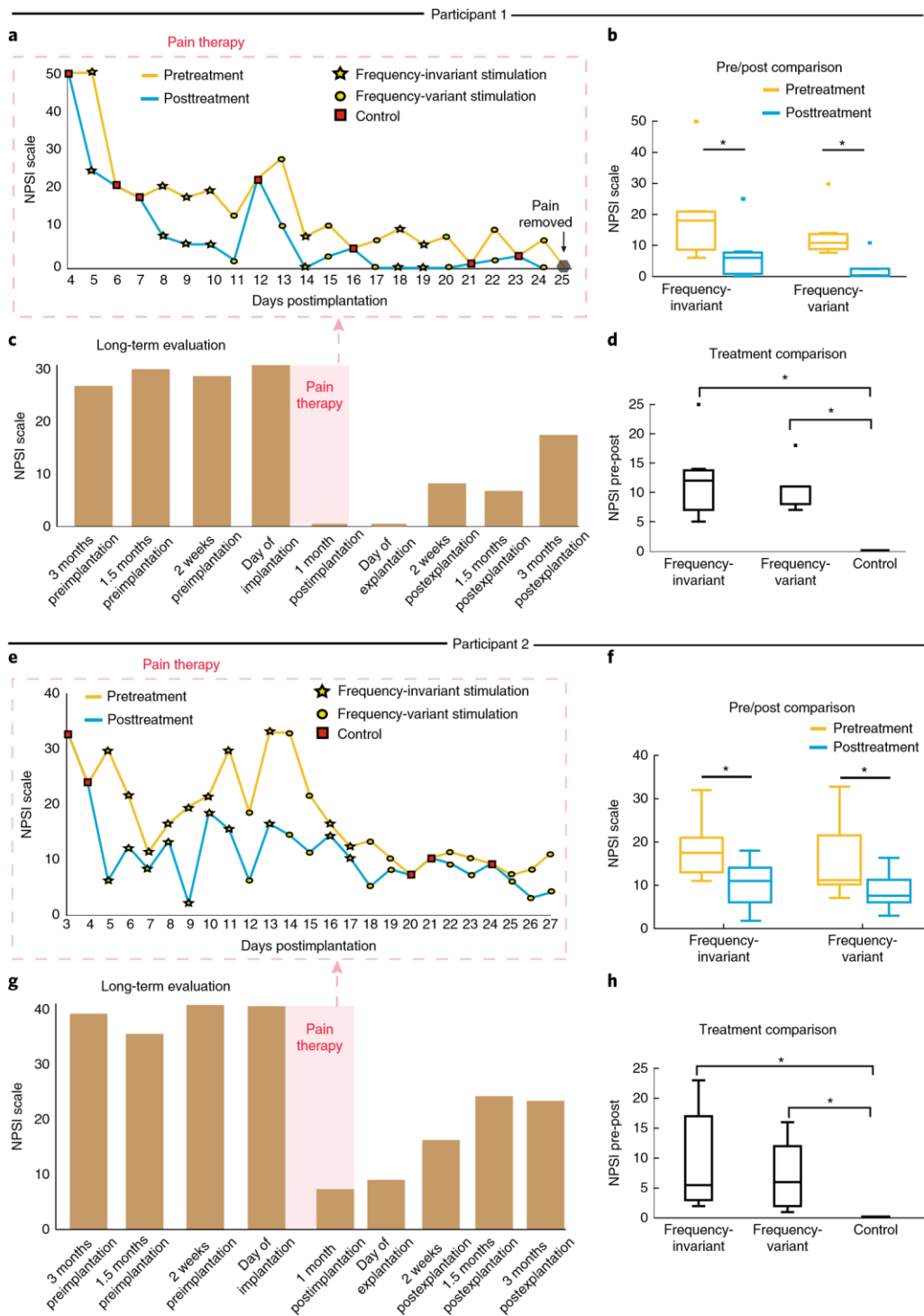


**Fig. 4 | Pain treatments: NPSI measurement. a–h**, NPSI score during the sessions with frequency-invariant and frequency-variant stimulation treatments; the controls for participants 1 (a) and 2 (e) are shown. Comparison between NPSI scores before and after the different treatments is shown for participants 1 (b) and 2 (f). The NPSI evolution over the weeks is shown for participants 1 (c) and 2 (g). A comparison of pain treatments for participants 1 (d) and 2 (h) is also shown. In each box plot, the thick horizontal line denotes the median, the lower and upper hinges correspond to the first and third quartiles, the whiskers extend from the hinge to the most extreme value no further than  $1.5 \times$  interquartile range from the hinge and the dots beyond the whiskers are outliers. Statistical evaluations were performed using a Kruskal–Wallis test with Tukey–Kramer correction for multigroup comparison. For participant 1, the average reduction in NPSI from before to after treatments was significant for frequency-invariant stimulation ( $n = 7$  stimulation sessions, d.f. = 1,  $P = 0.03$ ,  $\chi^2 = 4.24$ ) and for frequency-variant stimulation ( $n = 7$  stimulation sessions, d.f. = 1,  $P = 0.03$ ,  $\chi^2 = 7.41$ ) as was the case for participant 2 ( $n = 10$  stimulation



sessions for frequency-invariant stimulation, d.f. = 1,  $P = 0.008$ ,  $\chi^2 = 7.03$ ;  $n = 10$  stimulation sessions for frequency-variant stimulation, d.f. = 1,  $P = 0.02$ ,  $\chi^2 = 4.83$ ).

In **d**,  $P_{\text{frequency-invariant-frequency-variant}} = 0.91$ ,  $P_{\text{frequency-invariant-control}} = 0.0018$ ,  $P_{\text{frequency-variant-control}} = 0.0068$ , d.f. = 2,  $\chi^2_{\text{frequency-invariant-frequency-variant}} = 8.9$ ,  $\chi^2_{\text{frequency-invariant-control}} = 18.76$ ,  $\chi^2_{\text{frequency-variant-control}} = 17.47$ ; in **h**,  $P_{\text{frequency-invariant-frequency-variant}} = 0.93$ ,  $P_{\text{frequency-invariant-control}} = 0.00014$ ,  $P_{\text{frequency-variant-control}} = 0.00057$ , d.f. = 2,  $\chi^2_{\text{frequency-invariant-frequency-variant}} = 10.33$ ,  $\chi^2_{\text{frequency-invariant-control}} = 24.68$ ,  $\chi^2_{\text{frequency-variant-control}} = 23.38$ . \* $P < 0.05$ .

## Online content

Any methods, additional references, Nature Research reporting summaries, source data, statements of code and data availability and associated accession codes are available at <https://doi.org/10.1038/s41591-019-0567-3>.

Received: 8 March 2019; Accepted: 31 July 2019;

Published online: 9 September 2019

## References

1. Nolan, L. et al. Adjustments in gait symmetry with walking speed in trans-femoral and trans-tibial amputees. *Gait Posture* **17**, 142–151 (2003).
2. Miller, W. C., Deathe, A. B., Speechley, M. & Koval, J. The influence of falling, fear of falling, and balance confidence on prosthetic mobility and social activity among individuals with a lower extremity amputation. *Arch. Phys. Med. Rehabil.* **82**, 1238–1244 (2001).
3. Waters, R. L., Perry, J., Antonelli, D. & Hislop, H. Energy cost of walking of amputees: the influence of level of amputation. *J. Bone Joint Surg. Am.* **58**, 42–46 (1976).
4. Williams, R. M. et al. Does having a computerized prosthetic knee influence cognitive performance during amputee walking? *Arch. Phys. Med. Rehabil.* **87**, 989–994 (2006).
5. Flor, H., Nikolajsen, L. & Staehelin Jensen, T. Phantom limb pain: a case of maladaptive CNS plasticity? *Nat. Rev. Neurosci.* **7**, 873–881 (2006).
6. Makin, T. R. et al. Phantom pain is associated with preserved structure and function in the former hand area. *Nat. Commun.* **4**, 1570 (2013).
7. Boretius, T. et al. A transverse intrafascicular multichannel electrode (TIME) to interface with the peripheral nerve. *Biosens. Bioelectron.* **26**, 62–69 (2010).
8. Hargrove, L. J., Young, A. J. & Simon, A. M. Intuitive control of a powered prosthetic leg during ambulation: a randomized clinical trial. *J. Vasc. Surg.* **63**, 1405–1406 (2016).
9. Clites, T. R. et al. Proprioception from a neurally controlled lower-extremity prosthesis. *Sci. Transl. Med.* **10**, eaap8373 (2018).
10. Crea, S., Edin, B. B., Knaepen, K., Meeusen, R. & Vitiello, N. Time-discrete vibrotactile feedback contributes to improved gait symmetry in patients with lower limb amputations: case series. *Phys. Ther.* **97**, 198–207 (2017).
11. Rusaw, D., Hagberg, K., Nolan, L. & Ramstrand, N. Can vibratory feedback be used to improve postural stability in persons with transtibial limb loss? *J. Rehabil. Res. Dev.* **49**, 1239–1254 (2012).
12. Dietrich, C. et al. Leg prosthesis with somatosensory feedback reduces phantom limb pain and increases functionality. *Front. Neurol.* **9**, 270 (2018).
13. Petrini, F. M. et al. Six-month assessment of a hand prosthesis with intraneural tactile feedback. *Ann. Neurol.* **85**, 137–154 (2019).
14. Raspopovic, S. et al. Restoring natural sensory feedback in real-time bidirectional hand prostheses. *Sci. Transl. Med.* **6**, 222ra19 (2014).
15. Charkhkar, H. et al. High-density peripheral nerve cuffs restore natural sensation to individuals with lower-limb amputations. *J. Neural Eng.* **15**, 056002 (2018).
16. Clippinger, F. W., Seaber, A. V., McElhaney, J. H., Harrelson, J. M. & Maxwell, G. M. Afferent sensory feedback for lower extremity prosthesis. *Clin. Orthop. Relat. Res.* **169**, 202–206 (1982).
17. Tan, D. W. et al. A neural interface provides long-term stable natural touch perception. *Sci. Transl. Med.* **6**, 257ra138 (2014).
18. Rossini, P. M. et al. Double nerve intraneural interface implant on a human amputee for robotic hand control. *Clin. Neurophysiol.* **121**, 777–783 (2010).
19. Cruccu, G. et al. EFNS guidelines on neurostimulation therapy for neuropathic pain. *Eur. J. Neurol.* **14**, 952–970 (2007).
20. Wickens, C. D., Isreal, J. & Donchin, E. The event related cortical potential as an index of task workload. In *Proc. of the Human Factors and Ergonomics Society Annual Meeting* 282–286 (SAGE Publications, 1977).
21. Zink, R., Hunyadi, B., Van Huffel, S. & De Vos, M. Mobile EEG on the bike: disentangling attentional and physical contributions to auditory attention tasks. *J. Neural Eng.* **13**, 046017 (2016).
22. Isreal, J. B., Wickens, C. D., Chesney, G. L. & Donchin, E. The event-related brain potential as an index of display-monitoring workload. *Hum. Factors* **22**, 211–224 (1980).
23. Wickens, C., Kramer, A., Vanasse, L. & Donchin, E. Performance of concurrent tasks: a psychophysiological analysis of the reciprocity of information-processing resources. *Science* **221**, 1080–1082 (1983).
24. Burkitt, A. N. A review of the integrate-and-fire neuron model: I. homogeneous synaptic input. *Biol. Cybern.* **95**, 1–19 (2006).
25. Valle, G. et al. Biomimetic intraneural sensory feedback enhances sensation naturalness, tactile sensitivity, and manual dexterity in a bidirectional prosthesis. *Neuron* **100**, 37–45.e7 (2018).
26. Melzack, R. & Casey, K. L. Sensory, motivational, and central control determinants of pain: a new conceptual model. In *Proc. of the First International Symposium on the Skin Senses* (ed. Kenshalo, D. R.) 423–436, (Charles C Thomas Publisher, 1968).
27. Bouhassira, D. et al. Development and validation of the Neuropathic Pain Symptom Inventory. *Pain* **108**, 248–257 (2004).
28. Wewers, M. E. & Lowe, N. K. A critical review of visual analogue scales in the measurement of clinical phenomena. *Res. Nurs. Health* **13**, 227–236 (1990).
29. Orendurff, M. S. et al. Gait efficiency using the C-Leg. *J. Rehabil. Res. Dev.* **43**, 239–246 (2006).
30. Peduzzi de Castro, M., Soares, D., Mendes, E. & Machado, L. Plantar pressures and ground reaction forces during walking of individuals with unilateral transfemoral amputation. *PM R* **6**, 698–707.e1 (2014).
31. Gailey, R. et al. Unilateral lower-limb loss: prosthetic device use and functional outcomes in servicemembers from Vietnam war and OIF/OEF conflicts. *J. Rehabil. Res. Dev.* **47**, 317–331 (2010).
32. Naschitz, J. E. & Lenger, R. Why traumatic leg amputees are at increased risk for cardiovascular diseases. *QJM* **101**, 251–259 (2008).
33. Modan, M. et al. Increased cardiovascular disease mortality rates in traumatic lower limb amputees. *Am. J. Cardiol.* **82**, 1242–1247 (1998).
34. Johansson, J. L., Sherrill, D. M., Riley, P. O., Bonato, P. & Herr, H. A clinical comparison of variable-damping and mechanically passive prosthetic knee devices. *Am. J. Phys. Med. Rehabil.* **84**, 563–575 (2005).
35. Schmalz, T., Blumentritt, S. & Jarasch, R. Energy expenditure and biomechanical characteristics of lower limb amputee gait: the influence of prosthetic alignment and different prosthetic components. *Gait Posture* **16**, 255–263 (2002).
36. Genin, J. J., Bastien, G. J., Franck, B., Detrembleur, C. & Willems, P. A. Effect of speed on the energy cost of walking in unilateral traumatic lower limb amputees. *Eur. J. Appl. Physiol.* **103**, 655–663 (2008).
37. Detrembleur, C., Vanmarsenille, J.-M., De Cuyper, F. & Dierick, F. Relationship between energy cost, gait speed, vertical displacement of centre of body mass and efficiency of pendulum-like mechanism in unilateral amputee gait. *Gait Posture* **21**, 333–340 (2005).
38. Farrar, J. T., Young, J. P. Jr., LaMoreaux, L., Werth, J. L. & Poole, R. M. Clinical importance of changes in chronic pain intensity measured on an 11-point numerical pain rating scale. *Pain* **94**, 149–158 (2001).
39. Melzack, R. & Wall, P. D. Pain mechanisms: a new theory. *Science* **150**, 971–979 (1965).
40. Raspopovic, S., Petrini, F. M., Zelechowski, M. & Valle, G. Framework for the development of neuroprostheses: from basic understanding by sciatic and median nerves models to bionic legs and hands. *Proc. IEEE Inst. Electr. Electron. Eng.* **105**, 34–49 (2017).

## Acknowledgements

The authors are deeply grateful to the study participants who freely donated months of their life for the advancement of knowledge and for a better future for traumatic leg amputees. Thanks are also due to T. Palibrk for helping during the surgical implantation/explantation of the TIMEs and M. Marazzi for helping during the data analysis. European Research Council grant no. 759998 (FeelAgain), European Commission grant no. 754497 (SensAgain) and Swiss National Science Foundation grant no. 176006 (SYMBIO-LEG) funded this research.

## Author contributions

F.M.P. designed the study, developed the software and the overall system integration, performed and supervised the experiments, analyzed the data and wrote and reviewed the paper. M.B. performed the surgeries, was responsible for all the clinical aspects of the study and reviewed the manuscript. G.V. developed the software and the overall system integration, performed the experiments, analyzed the data and reviewed the manuscript. V.I. and S. Mazic collected and analyzed the metabolic measurements. P.M. and B.M. collected and analyzed the EEG measurements. P.C. and T.S. developed the TIME electrodes and delivered technical assistance during the implantation and explanation procedures. F.B. and D.B. developed the software and the overall system integration and performed the experiments. N.K. analyzed the data. D.G. and D.A. designed the hardware and embedded software (real-time control) for STIMEP. K.L. and A.A. participated in the experimental design, prosthesis fitting and system integration, discussed the results and reviewed the manuscript. A.L. assisted with the surgeries, selected the participants and managed the regulatory pathway and clinical aspects. S. Micera designed the study, discussed the results and wrote the manuscript. S.R. designed the study, performed and supervised the experiments, managed the regulatory pathway, coanalyzed the data and wrote the manuscript. All authors had access to the relevant data. All authors authorized submission of the manuscript; the final submission decision was taken by the corresponding author.

## competing interests

F.M.P., S.R. and S. Micera hold shares of SensArs Neuroprosthetics Sarl, a start-up company dealing with the commercialization of neurocontrolled artificial limbs. The other authors declare no competing interests.

## Additional information

**Extended data** is available for this paper at <https://doi.org/10.1038/s41591-019-0567-3>.

**Supplementary information** is available for this paper at <https://doi.org/10.1038/s41591-019-0567-3>.

**Reprints and permissions information** is available at

[www.nature.com/reprints](http://www.nature.com/reprints). **Correspondence and requests for materials** should be addressed to S.R.

**Peer review information:** Brett Benedetti was the primary editor on this article and managed its editorial process and peer review in collaboration with the rest of the editorial team.

**Publisher's note:** Springer Nature remains neutral with regard to jurisdictional claims in published maps and institutional affiliations.

© The Author(s), under exclusive licence to Springer Nature America, Inc. 2019

## Methods

**Study design.** All participants were assigned to the same intervention (provision of sensory feedback restored by nerve stimulation delivered through implanted nerve interfaces), which was controlled (no provision of sensory feedback through nerve stimulation). Intervention and control conditions were presented in a random order.

The random sequence was created through the randperm function in MATLAB vR2016b (MathWorks). Control and intervention conditions were balanced. The random sequence was determined before each task by the experimenter.

**Participants.** Participants provided signed informed consent before inclusion in the study. The study was approved by the ethical committee of the Clinic Center of Serbia and the national competent authorities. Three individuals with unilateral transfemoral amputation were recruited according to the following inclusion criteria: (1) K4 users of prostheses (Supplementary Material); (2) affected by drug-resistant PLP before the study. Three participants underwent surgery; however, due to work occupancy, one participant decided not to participate in the experiments, but took part in a limited number of other procedures. The first participant, a 49-year-old male, had undergone amputation 3 years before enrollment in the study because of a work accident. The second participant, a 35-year-old male, had undergone amputation 12 years previously because of a car accident. The demographic characteristics of the participants are shown in Supplementary Table 1. All participants read and signed the informed consent. They were also informed about the research nature of the procedure where the outcome would be uncertain. The trial was registered with ClinicalTrials.gov (NCT03350061). All participants were proficient users of a prosthesis (3R80; Ottobock).

**Procedures. Surgery.** The implantation of the electrodes was performed under general anesthesia. The incision for electrode insertion was made over the sulcus, between the biceps femoris and semitendinosus muscles, in the middle of the posterior aspect of the thigh, starting approximately 4.5 cm proximally to the end of the amputation stump. To identify the sciatic nerve, the semitendinosus muscle was moved medially and the biceps femoris was moved laterally. Participants were implanted with five TIME-4H electrodes, four in the tibial branch of the sciatic nerve (the target) and one in the peroneal branch, following the same insertion procedure (Extended Data Fig. 1). This was done to avoid the (remote) possibility of anatomical variant where the tibial nerve was switched with the peroneal nerve. First, a small window was made in the epineurium, which was used by the surgeon to transversally cross the various visible fascicles. Thus, the electrode was pulled through the nerve and its active (stimulating) sites were placed in contact with the nerve fascicles. When the electrode had been positioned, it was fastened to the epineurium with a suture through its specific fixation tabs. Once all the electrodes had been implanted, a flap was raised by cutting a patch of fascia and wrapping it around the electrode cables. The flap was then sutured to the underlying tissue. Finally, the cables were tunneled through the thigh and pulled out of the leg through small incisions (for each cable, a small skin incision was cut) made on the anterolateral aspect, just a few centimeters below the iliac crest. This enabled transcutaneous connection with an external neurostimulator. The stimulator embedded the impedance check feature used during the surgery and entire experimentation. After every implantation, a contact (electrodes' active sites) check took place to verify that the impedance of the active sites was <100 kOhm, meaning potential functionality (capability of injecting charge in the nerve). Surgeries lasted around 4 h. At end of the study, both participants had the electrodes removed.

**Sensation characterization.** Two days after implantation, the participants' responses to the stimulation were characterized (mapped). During each mapping session, up to 4 electrodes (14 active sites each) were connected to the neural stimulator (STIMEP; Axonic and Inria, University of Montpellier). STIMEP delivered trains of biphasic balanced cathodic-first pulses of electrical currents with a variable intensity, duration and frequency, between the electrode active site(s) and the electrode ground. An operator managed the device using custom-made software. The intensity of the pulses ranged from 10 to 980  $\mu$ A with a resolution of a minimum of 10  $\mu$ A, while pulse length was fixed in a range from 10 to 120  $\mu$ s, depending on the active site and frequency (50 Hz, as in our previous study<sup>14</sup>); 1-s pulse trains were delivered. The interval between trains was 2 s. Participants described the sensations elicited by the intraneural stimulation, reporting their type, extent, intensity and location. A graphical user interface was purposely developed for use in this trial. Through this software, the reports of participants were recorded as well as the parameters of the stimulation injected into the neural electrodes. For the sensation types, participants could choose from a list of items (similar to the one of Kim et al.<sup>41</sup>) but also propose new descriptions if needed, to avoid the risk of forcing them to associate a sensation with the requirements of the test. Location and extent could be drawn on an illustration of

the foot and leg. Intensity was reported on a scale from 0 to 10 (as in Petrini et al.<sup>15</sup>). Participants could also freely make a description of the elicited sensation, if needed.

**Neuroprosthesis.** After the first month, users were fitted with the prosthesis, provided by Össur. Accommodation time and instructions were adequately provided within a day. In fact, the functions of a newly fitted prosthetic component can be intuitively used after a few hours of adaptation time if the motion patterns required are similar to those of the previous fitting<sup>42</sup>. The neuroprosthesis consisted of the intraneural electrodes (IMTEK), the stimulator (Inria), an external controller and a sensorized insole (SensArs Neuroprosthetics), located under a custom made transfemoral prosthesis (composed of commercially available prosthetic components: RHEO KNEE XC, PRO-FLEX XC foot and transfemoral flexible brim socket fitted to an Iceross Seal-In X5 TF silicon liner, Ossur hf, Iceland). The microprocessor-controlled knee has an integrated knee encoder and the knee angle could be communicated with 1° resolution via Bluetooth. The insole had a substrate of fabric on which seven pressure sensors were distributed. The resolution of the sensors was 0.05 kg and the maximum measurable weight was 100 kg for each of them. The sampling frequency of the acquisition and amplification system of the sensorized sole was 75 Hz. The system also had a Bluetooth module. The external controller was implemented on a Raspberry Pi 3 (Raspberry Pi Foundation). This communicated through a serial peripheral interface (wired link) with the stimulator that embedded the firmware<sup>43</sup> (low-level safety procedures, stimulus generation, real-time modulation and impedance measurements), and via Bluetooth with the sensorized sole and knee encoder. The portable microprocessor controlled the recording and acquisition of sensor readouts and transduced them into stimulation parameters through sensory encoding algorithms. The process of acquisition, recording and encoding lasted 50 ms. The neurostimulator and external controller were placed in a small backpack carried by each participant. The results from the mapping procedure were used to couple the sensors with the active sites, thereby eliciting a sensation in the phantom area corresponding to the position of the sensors themselves. The readouts of three of the insole pressure sensors and the knee encoder were used as control inputs for the intraneural stimulation of four active sites. An active site eliciting a sensation in the central metatarsus, one in the lateral metatarsus, one in the heel and one eliciting a sensation in the calf (interpreted as knee flexion) were used for each participant (Fig. 1). The amplitude of the stimulation pulses injected into a set of four targeted active sites was controlled independently in real-time according to a linear relationship. The same setup was used for each participant. The amplitude of biphasic, symmetric, cathodic-first and rectangular chargebalanced pulses was modulated according to the following linear relationship:

$$c = \frac{1}{4} \frac{\delta c_{\max} - c_{\min}}{\delta s_{50} - s_0} (s - s_0) + c_{\min} \quad \text{whens} \leq s_0 \leq s_{50} \leq s_{\max}$$
$$c = \frac{1}{4} c_{\max} \quad \text{whens} > s_{\max}$$

where  $c$  is the amplitude of the stimulation train,  $s$  is the sensor readout,  $s_0$  and  $s_{\max}$  represent the minimum and maximum pressure applied during walking by the individual in the case of the sensorized sole and 10 and 55 degrees for the encoder;  $c_{\min}$  and  $c_{\max}$  are the stimulation amplitudes that evoked the minimum (that is, perceptual threshold) and maximum (that is, below pain threshold) sensations, respectively, as reported by each participant according to the mapping procedure. The frequency was fixed at 50 Hz<sup>14</sup>.

The types of sensations used in the neuroprosthesis for the foot were touch, pressure and vibration; for the knee, it was an activation of the phantom calf.

**Outcomes.** Walking speed, confidence, metabolic consumption and mental effort were tested starting from one month after the electrodes were implanted, while pain treatment was administered during the first month after implantation.

**Metabolic consumption evaluation.** A mobile spirometry system (Oxycon Mobile; Erich Jaeger, VIASYS Healthcare), equipped with wireless telemetry to a computer, was used to measure oxygen consumption. The rate of oxygen uptake ( $\text{VO}_2$ ) was then calculated by dividing oxygen consumption by the mass of each participant.

All parameters were recorded in 5-s increments and processed using personal computer software (JLAB 5.72; CareFusion 234 GmbH). Device calibration was performed before each recording, according to the standard procedures recommended by the manufacturer's manual, using the automatic ambient, volume and gas calibration functions. The gas analyzer was calibrated using a standard gas mixture at 180 kPa:  $\text{O}_2 = 16.25\%$ ;  $\text{CO}_2 = 4.13\%$ ; rest  $\text{N}_2$ .

Tests were performed both indoors and outdoors. All testing protocols were conducted with and without sensory feedback in random order. Rests between trials were taken as needed. Laboratory testing was performed on a motorized

treadmill (T170; COSMED). After 15 min of familiarization with walking on the treadmill and a 10-min rest, each participant started the test by standing on a treadmill for 3 min while the cardiorespiratory parameters were recorded. Then, without a vertical gradient, the treadmill speed was increased by 0.5 km h<sup>-1</sup> every minute for as long as the participants could maintain normal walking kinematics or refused to proceed because of feelings of exhaustion or fear of falling. The VO<sub>2</sub> per speed was obtained by averaging the recordings during the minute of walking at that speed.

Outdoor walking was performed on grass. After 3 min of collecting baseline resting gas exchange data, participants started the test by walking at a self-selected speed. To reach and maintain a steady state, this phase lasted 6 min and data from the last 3 min were averaged to calculate the cardiorespiratory response. We measured gait efficiency through gross and net VO<sub>2</sub>. Gross VO<sub>2</sub> was calculated as steady state VO<sub>2</sub> normalized with regard to speed, while net VO<sub>2</sub> was calculated as the difference between steady state and resting VO<sub>2</sub> scaled to the speed (ml O<sub>2</sub> kg<sup>-1</sup> m<sup>-1</sup>).

**Walking speed and confidence assessment.** During the outdoor experiments, participants were asked to walk on a sandy terrain. Experiments were configured in sessions of 1 min per condition. A rectangle (4.60 × 4.20 m) was traced on the ground and participants had to walk forming a figure of eight outside the rectangular area (Fig. 1). Tests were run randomly with and without sensory feedback. Both participants performed a total of 6 min × 2 sessions of tests per condition. The number of meters traveled during each trial was measured, as in other trials with prosthetic legs<sup>34</sup>. At the end of each repetition, participants were also asked to assess their own confidence while walking, using a number from 0 to 10. We adopted one item of the standard subjective rating confidence assessment scales available for clinical uses<sup>45,46</sup>.

**Mental effort assessment.** To assess the participants' mental effort while walking with and without sensory feedback, we employed a dual-task paradigm, consisting of a walking task on sand (primary task) and a three-tone auditory oddball task<sup>31</sup> (secondary task) performed simultaneously. The walking task was the same we described in the walking speed and confidence assessment section. The oddball task consisted of standard, target and deviant tones presented through headphones in a random order. The task consisted of a standard tone (900 Hz, appearing 80% of the time) and two deviant tones (600 Hz and 1,200 Hz, each appearing 10% of the time) lasting 80 ms with a mean interstimulus interval of 1,000 ms. The tones were presented to each participant in a random order and played binaurally through headphones. To prevent participants from getting used to the task, we added a jitter timing of ±200 ms to the interstimulus interval. Participants had to silently count the target tones and ignore the standard and deviant tones, while walking over sand with or without the intraneural sensory feedback. Participants' attention to an attended (target) tone was expected to elicit distinguishably higher P300 amplitude versus the nonattended (deviant and standard) tones. Participants received a balanced number of tones in every condition; thus, the task lasted the same time in every condition. The traveled distance in both conditions was similar for both participants (208 m with and without intraneural feedback for participant 1, and 249.6 m with intraneural feedback versus 228.8 m without feedback for participant 2).

The Presentation Mobile app (Neurobehavioral Systems) was used for stimulus presentation and synchronization with the EEG data. The software sends the time stamps of the auditory tones with millisecond precision to the EEG acquisition software (SMARTING Android app) through an open source lab streaming layer protocol (<https://github.com/scn/labstreaminglayer>), so that EEG and auditory tones data can be fully synchronized and recorded in XDF file format. The software was run on an Android smartphone (Sony Xperia Z1) to which the headphones were attached. The SMARTING mobile EEG amplifier was streaming the acquired data wirelessly to the same Android phone via a Bluetooth connection. EEG data acquisition was performed using the SMARTING wireless EEG system (mBrainTrain), with a sampling frequency of 500 Hz and 24-bit data resolution. Data were streamed in real-time to the SMARTING android app and recorded in a file. The small and lightweight EEG amplifier was tightly connected to a 24-channel electrode cap (EASYCAP) at the occipital site of the participants' head, using an elastic band. The design of the cap-amplifier unit ensured minimal isolated movement of individual electrodes, cables or amplifier; this strongly reduced movement artifacts. Furthermore, the small dimensions of the recording system provided full mobility and comfort to the participants. The electrode cap contained sintered Ag/AgCl electrodes that were placed based on the international 10–20 system: Fp1, Fp2, Fz, F7, F8, FC1, FC2, Cz, C3, C4, T7, T8, CPz, CP1, CP2, CP5, CP6, TP9, TP10, Pz, P3, P4, O1 and O2. The electrodes were referenced to the FCz and the ground electrode was AFz. Before the experiments started, the procedure chosen required that electrode impedances must be below 5 kΩ; this was confirmed by the device acquisition software.

The participants' attention to the target tones was expected to elicit a distinguishable P300 ERP component<sup>47</sup> higher than the ones due to deviant and standard tones. The hypothesis<sup>31</sup> was that the more mental power consumed by

walking, the lower the evoked P300 amplitude during the auditory oddball task, indicating a reduced availability of mental resources. A higher P300 amplitude corresponds to the ability of an individual to allocate enough mental resources to process the information of the stimuli during dual-task performance<sup>30</sup>. (The auditory oddball task represents the secondary task, while walking is the primary task.) In this particular experiment, the higher P300 amplitude obtained on the target tones (compared to the P300 amplitude on the deviant ones) should correspond to lower mental effort of the primary task (walking), meaning that the P300 amplitude is inversely correlated with the easiness to walk—the higher the P300 component on the target tones (and significantly different from the higher P300 component on the deviant ones), the easier the walking. The oddball paradigm (both auditory or visual) has already been used to assess secondary task performance, for example, assessing distraction while driving<sup>48</sup>, measuring workload for display workers<sup>22</sup>, investigating the ability of pilots to pay attention to the auditory alarms in the cabin during landing<sup>49</sup> and quantify the mental workload of prosthesis control during human-machine interaction<sup>50</sup>.

EEG signal processing was analyzed offline using EEGLAB v14 and MATLAB v2016b (MathWorks). As the preprocessing step, EEG data were bandpassfiltered in the 1–30 Hz range, followed by an artifact subspace reconstruction algorithm to remove artifacts that mostly originated from walking<sup>51</sup>. Further, signals were re-referenced to the average of the mastoid channels (Tp9 and Tp10). To semiautomatically remove nonphysiological artifacts such as eye blinks and eye motion, an extended infomax independent component analysis was executed<sup>52</sup>. After data preprocessing, ERP epochs were extracted from –200 to 800 ms with regard to the time stamp values of the auditory stimuli indicated by the Presentation Mobile app. Baseline values were corrected by subtracting the mean values for the period from –200 to 0 ms from the stimuli. Finally, ERPs with extreme amplitude values (±100 μV) were rejected from further analyses. The electrode site of interest for the ERP analysis was the Pz electrode, since the P300 component is the most prominent over the parietocentral scalp location<sup>47</sup>. Depending on the experiment, the 'target' and 'deviant' stimuli were either the 600 or 1,200 Hz tones. The grand average ERPs across participants were computed for both target and nontarget conditions. Furthermore, the P300 amplitude was calculated for both target and deviant (nontarget) conditions and for each experimental condition, using mean amplitude measures<sup>53</sup> in the time window from 450 to 650 ms, with regard to the time stamps of the stimuli. Finally, statistical analysis of the results was carried out.

**Pain treatment.** Pain treatment was conducted during the first month of tests after the electrode implantation to avoid interference with prosthesis use.

Both participants received two different types of pain treatment: frequency-invariant and frequency-variant stimulation. During frequency-invariant stimulation, a 10-min train of stimulation with fixed frequency (50 Hz), amplitude and pulse-width (depending on the intensity of the sensation perceived) was delivered, eliciting a medium-intensity percept (3 or 4 on a scale of 0–10) spatially close to the painful area in the phantom foot. In the case of frequency-variant stimulation, the 10-min stimulation trains had fixed amplitude and pulse-width (depending on the intensity of the sensation perceived), but variable frequency, again eliciting a medium-intensity percept spatially close to the painful area in the phantom foot. The pulse frequency followed a Poisson distribution envelope (Extended Data Fig. 5). In both conditions, trains consisted of 2 s of stimulation and a 2-s pause, delivered while the prosthetic leg was detached. The frequency-invariant and frequency-variant paradigms were selected to reproduce the constant frequency stimulation pattern of commercial stimulators<sup>19</sup> for pain relief (the former) and the variable firing rate of human skin mechanoreceptors<sup>54</sup> (the latter). The modalities of the sensations were physiologically plausible ones (touch, pressure and vibration; Extended Data Fig. 2) and not electro-paresthesia, which is the modality commonly elicited by commercial stimulators<sup>19</sup> for pain relief. Participant 1 received 7 sessions per stimulation type (after which no further pain was reported), while participant 2 received 10 sessions per stimulation. Each session was tested in a different day (from day 4 to 25 postimplantation for participant 1 and from day 3 to 27 postimplantation for participant 2). Frequency-invariant and frequency-variant conditions were controlled with 10-min sessions of no stimulation (Fig. 4d,h and Extended Data Fig. 3d,h): participant 1 had 7 control sessions, while participant 2 only 5 because (1) he was frustrated with reporting no pain rating change when filling the questionnaire and (2) the 7 control sessions of participant 1 did not show any change in the reported pain level. The NPSI<sup>57</sup> and VAS<sup>58</sup> questionnaires used to assess pain were presented at three months, one and a half months, two weeks before electrode implantation, the day of implantation, before and after every therapeutic condition (frequency-invariant, frequency-variant and control), right before and after electrode explantation and up to three months after explantation (Fig. 4c,g and Extended Data Fig. 3c,g). The VAS consisted of a 4-item questionnaire; items represented pain (rated between 0 and 10) in the foot, calf, knee and thigh. The cumulative VAS was calculated by summing the score for each item (between 0 and 40); the NPSI ranged from 0 to 100.

**Statistical analysis.** No statistical methods were used to predetermine the size of the population of recruited participants because this study was designed as an initial proof-of-concept study to provide preliminary evidence of the benefits afforded to leg amputees by sensory feedback restored through direct nerve stimulation. The number of repetitions for each of the tests was determined as follows:

walking outdoor was designed on a standard 6-Minute Walk Test<sup>55</sup>; the mental effort assessment was designed by reproducing the dual task proposed by Zink et al.<sup>21</sup>;

Outdoor metabolic consumption was based on Waters et al.<sup>3</sup> and Steffen et al.<sup>55</sup>; Indoor metabolic consumption was inspired by Traballese et al.<sup>56</sup>;

Pain therapy was designed after the protocol of Sojin et al.<sup>57</sup>: we planned the measurements before implanting the electrodes, provided treatment therapies when participants reported uncomfortable pain (up to ten repetitions  $\times$  two conditions plus controls until one month after electrode implantation) and arranged follow-up.

The number of experiments with  $\alpha = 0.05$  guaranteed a statistical power for the two participants of 99% on average (with Cohen's  $d = 0.83$ ) for the outdoor metabolic consumption evaluation, 86% with an effect size of 0.83 ( $d = 0.57$ ) for the indoor metabolic consumption evaluation, 93% ( $d = 0.96$ ) for the outdoor walking speed test, 100% ( $d = 0.91$ ) for the outdoor walking confidence test, 71% ( $d = 0.26$ ) for the mental effort assessment, 88% ( $d = 0.65$ ) for the NPSI pain assessment and 87% ( $d = 0.64$ ) for the cumulative VAS pain assessment.

All data were analyzed offline in MATLAB vR2016b. Data are shown as mean values  $\pm$  s.d. or as the median and interquartile range (unless otherwise indicated). The normality of data distributions was determined with the Kolmogorov–Smirnov test. Statistical evaluations of sensation characterization, walking speed, walking confidence, metabolic cost and pain were performed on the basis of the Kolmogorov–Smirnov test results, using a one-way ANOVA or Kruskal–Wallis test. The specific statistical tests applied to the different experiments are shown in the figure legends. The Tukey–Kramer correction was applied in the case of multiple groups of data.

For the EEG signals, a  $2 \times 2$  ANOVA (sensory feedback/no feedback  $\times$  target/nontarget tones) was computed, along with a post hoc test (paired  $t$ -test) to compare multiple groups.

The significance level for all statistical tests was set at 0.05, unless otherwise stated in the figures.

**Reporting Summary.** Further information on research design is available in the Nature Research Reporting Summary linked to this article.

## Data availability

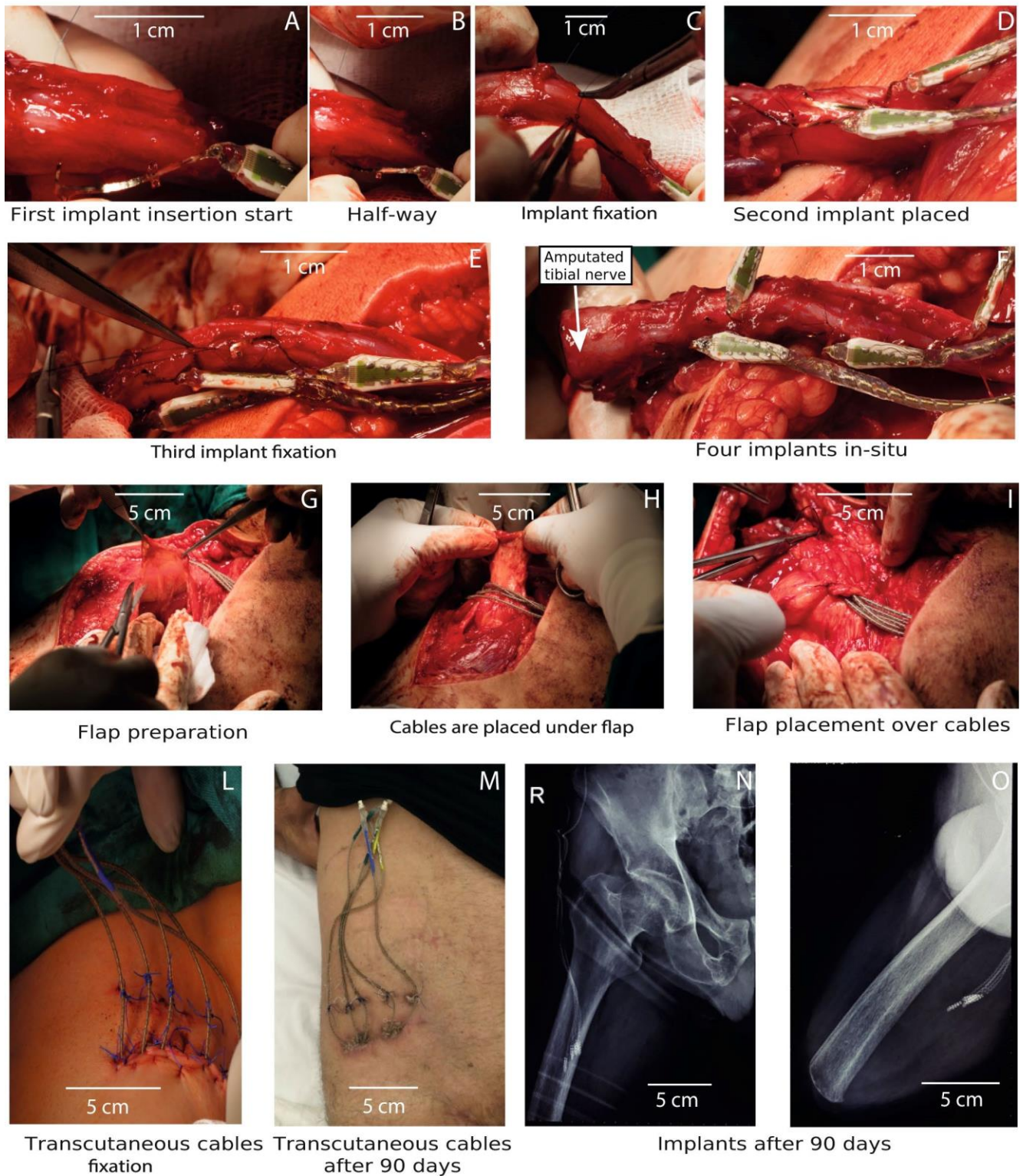
Data that support the findings and software routines developed for the analysis are available from the corresponding author. Data can be made available to qualified individuals for collaboration provided that a written agreement is signed in advance between the included consortium and the requester's affiliated institution.

## References

- Kim, L. H., McLeod, R. S. & Kiss, Z. H. T. A new psychometric questionnaire for reporting of somatosensory percepts. *J. Neural Eng.* **15**, 013002 (2018).
- Bellmann, M., Schmalz, T., Ludwigs, E. & Blumentritt, S. Immediate effects of a new microprocessor-controlled prosthetic knee joint: a comparative biomechanical evaluation. *Arch. Phys. Med. Rehabil.* **93**, 541–549 (2012).
- Andreu, D., Guiraud, D. & Souquet, G. A distributed architecture for activating the peripheral nervous system. *J. Neural Eng.* **6**, 026001 (2009).
- Hafner, B. J. & Smith, D. G. Differences in function and safety between Medicare Functional Classification Level-2 and -3 transfemoral amputees and influence of prosthetic knee joint control. *J. Rehabil. Res. Dev.* **46**, 417–433 (2009).
- Asano, M., Miller, W. C. & Eng, J. J. Development and psychometric properties of the ambulatory self-confidence questionnaire. *Gerontology* **53**, 373–381 (2007).
- Powell, L. E. & Myers, A. M. The Activities-specific Balance Confidence (ABC) Scale. *J. Gerontol. A Biol. Sci. Med. Sci.* **50A**, M28–M34 (1995).
- Polich, J. Updating P300: an integrative theory of P3a and P3b. *Clin. Neurophysiol.* **118**, 2128–2148 (2007).
- Strayer, D. L. et al. Assessing cognitive distraction in the automobile. *Hum. Factors* **57**, 1300–1324 (2015).
- Giraudet, L., St-Louis, M.-E., Scannella, S. & Causse, M. P300 event-related potential as an indicator of inattention deafness? *PLoS One* **10**, e0118556 (2015).
- Deeny, S., Chicoine, C., Hargrove, L., Parrish, T. & Jayaraman, A. A simple ERP method for quantitative analysis of cognitive workload in myoelectric prosthesis control and human-machine interaction. *PLoS One* **9**, e112091 (2014).
- Mullen, T. R. et al. Real-time neuroimaging and cognitive monitoring using wearable dry EEG. *IEEE Trans. Biomed. Eng.* **62**, 2553–2567 (2015).
- Viola, F. C. et al. Semi-automatic identification of independent components representing EEG artifact. *Clin. Neurophysiol.* **120**, 868–877 (2009).
- Luck, S. J. *An Introduction to the Event-related Potential Technique* (The MIT Press, 2014).
- Kennedy, P. M. & Inglis, J. T. Distribution and behaviour of glabrous cutaneous receptors in the human foot sole. *J. Physiol.* **538**, 995–1002 (2002).
- Steffen, T. M., Hacker, T. A. & Mollinger, L. Age- and gender-related test performance in community-dwelling elderly people: Six-Minute Walk Test, Berg Balance Scale, Timed Up & Go Test, and gait speeds. *Phys. Ther.* **82**, 128–137 (2002).
- Traballese, M., Porcacchia, P., Averna, T. & Brunelli, S. Energy cost of walking measurements in subjects with lower limb amputations: a comparison study between floor and treadmill test. *Gait Posture* **27**, 70–75 (2008).
- Sojin, A., Syed Shah, N. & Fang, Z.-P. High-Frequency electrical nerve block for postamputation pain: a pilot study. *Neuromodulation* **18**, 197–206 (2015).

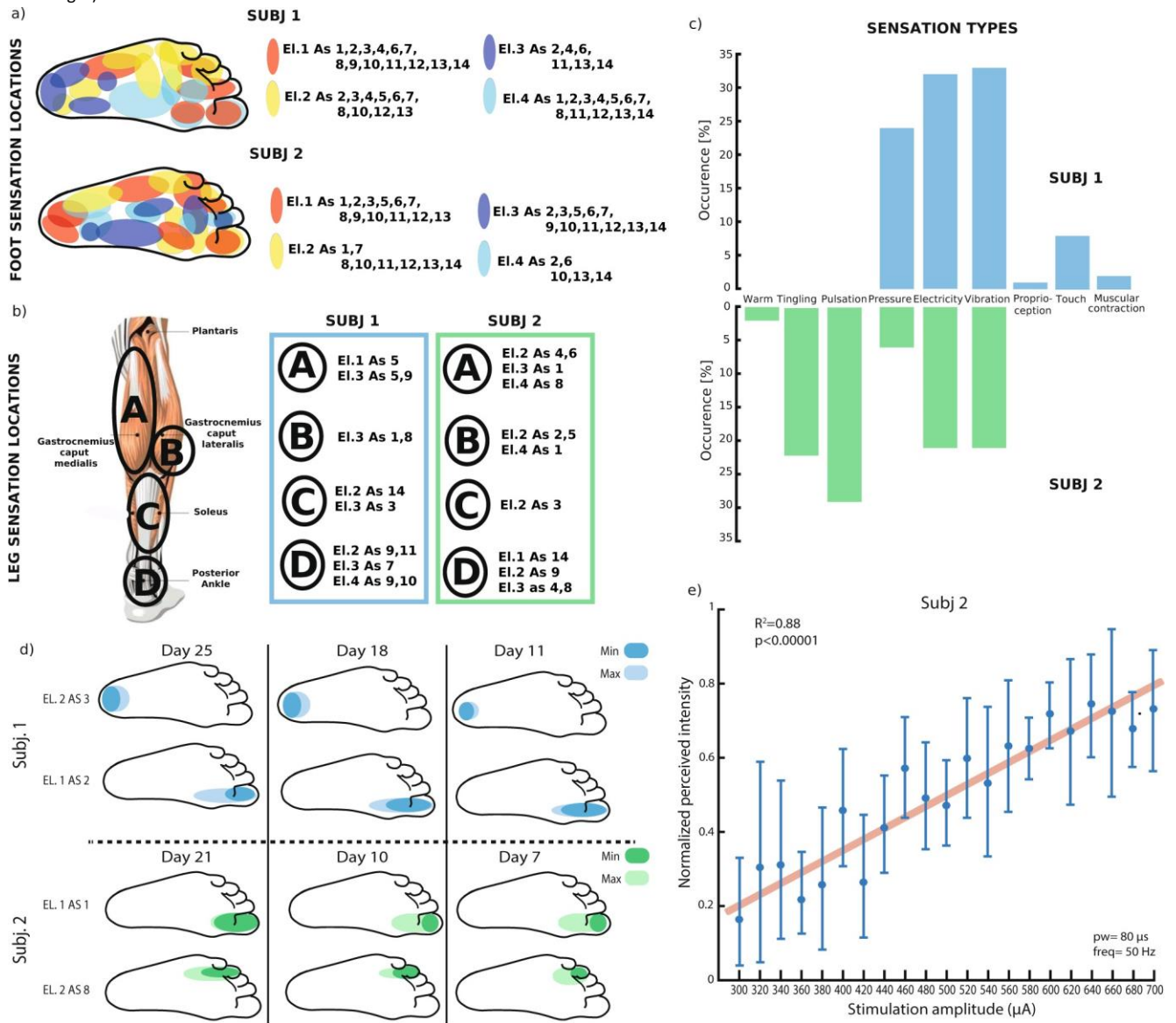


Surgical procedure: insertion of implants into the tibial nerve and their stabilisation



**Extended Data Fig. 1 | Surgical implantation of the neural interfaces.** After the nerve dissection from the surrounding tissues, a small window is opened on the nerve epineurium, exposing different fascicles, which can be visualized. The implants are placed by carefully pulling the guiding needle, which is connected to the electrodes. The implants are positioned to cross the majority of fascicles in a very close (longitudinal) space. Cables are fixed by flap preparation from the fascia tissue. The electrode cables are tunneled through the thigh and

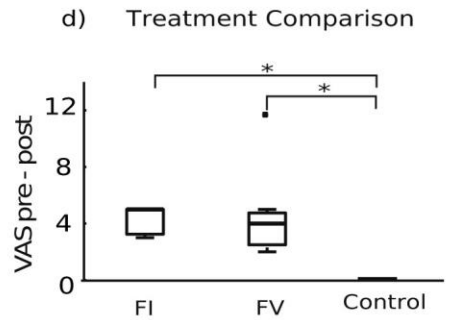
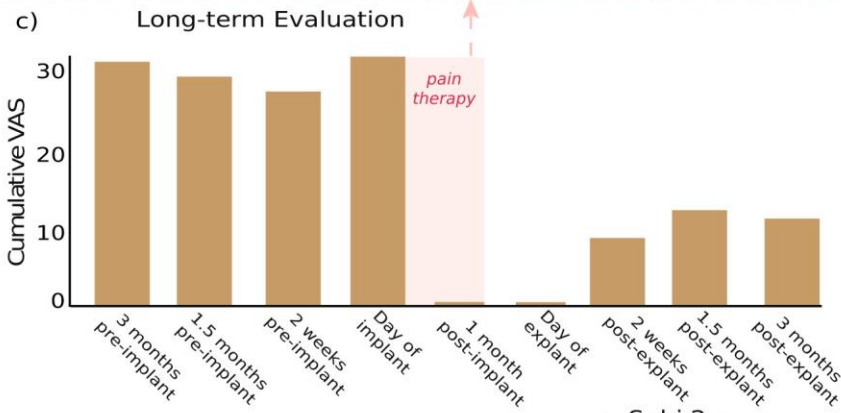
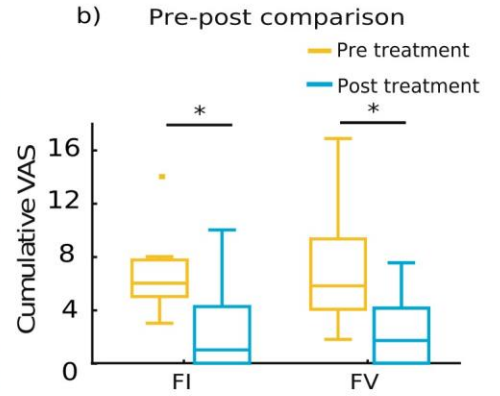
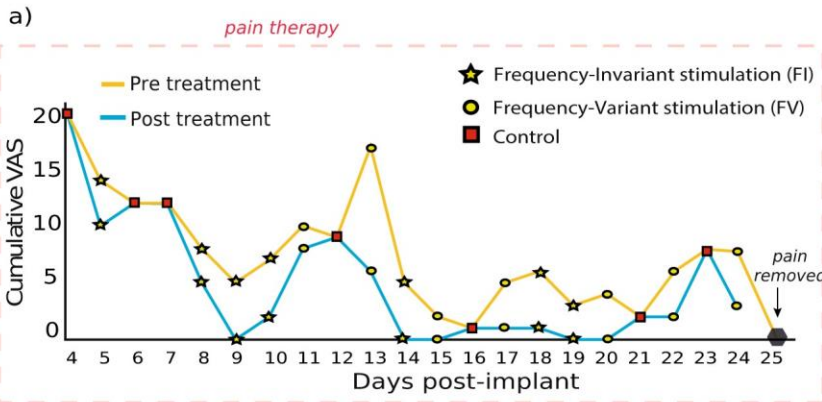
pulled out of the leg through small incisions (for each cable, a small skin incision is made) just a few centimeters below the iliac crest, to enable transcutaneous connection with the neurostimulator. Electrode positioning is shown in the X-ray pictures taken before explantation (bottom right).



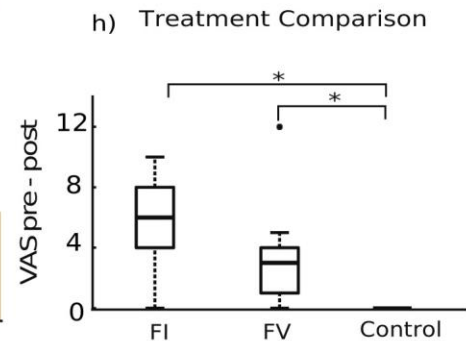
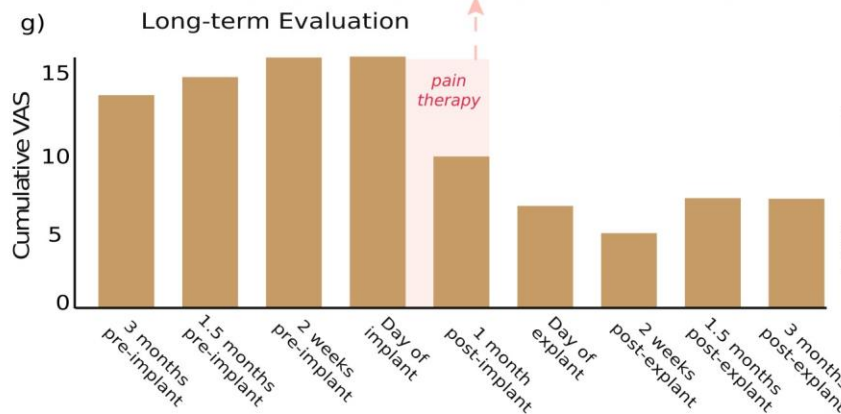
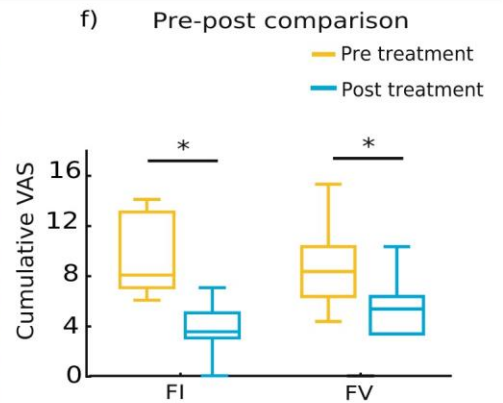
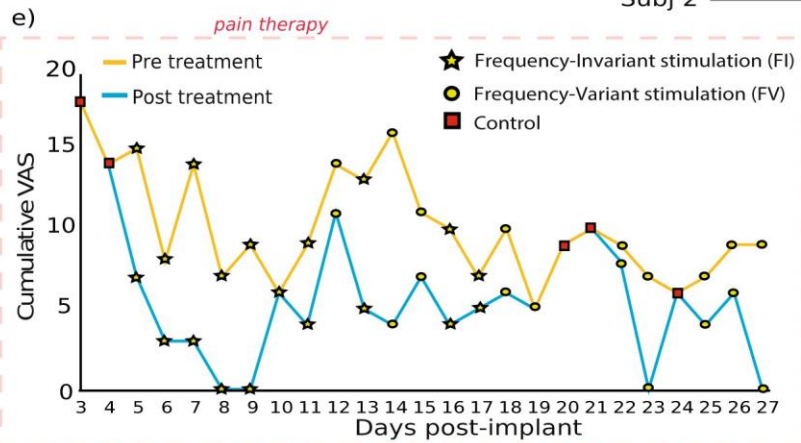
**Extended Data Fig. 2 | Sensation characterization.** The sensation characterization process is implemented to determine the response of the individual to the stimulation. **a**, Distribution of tactile sensations over the foot elicited by the stimulation of the four electrodes (color-coded). The number of electrode sites evoking a sensation in the foot is reported. **b**, Distribution of sensations over the lower leg (A, gastrocnemius caput medialis; B, gastrocnemius caput lateralis; C, soleus; D, posterior ankle). The number of active sites eliciting sensations is also reported. **c**, The percentage of sensation types reported during the trial for each participant is shown. **d**, The evoked sensation extension according to the minimum and maximum perceived intensity is displayed. Data are reported for three different days and two active sites in both participants. **e**, The proportional relationship between the amplitude of the injected pulses and the normalized perceived sensation intensity for participant 2 is shown. Pulse width and stimulation frequency are displayed. The points indicate the mean ratings ( $n = 6$  ramps of stimulation amplitudes); the error bars denote the s.d.; the faded line is the line of best fit. The coefficient of determination  $R^2$  and  $P = 5.7 \times 10^{-7}$  obtained from the Pearson correlation coefficient calculation (to test if the corresponding correlation  $R$  is considered significant) are reported.



Subj 1



Subj 2



**Extended Data Fig. 3 | see figure caption on next page.**

**Extended Data Fig. 3 | Pain treatments: cumulative VAS measurement. a–h,** A pain treatment session consisted of 10 min of stimulation.

Before and after the session, participants completed the cumulative VAS questionnaire. The cumulative VAS was also recorded over time

before and after the implant/explant. The VAS score during the sessions with frequency-invariant and frequency-variant stimulation

treatments, and the control are shown for participants 1 (a) and 2 (e). A comparison between the cumulative VAS score before and after the

different treatments is shown for participants 1 (b) and 2 (f). The cumulative VAS evolution over the weeks is shown in participants 1 (c), and 2

(g). A comparison of pain treatments for participants 1 (d) and 2 (h) is shown. In each box plot, the thick horizontal line denotes the median, the

lower and upper hinges correspond to the first and third quartiles, the whiskers extend from the hinge to the most extreme value no further

than  $1.5 \times$  interquartile range from the hinge and the dots beyond the whiskers are outliers. Statistical evaluations were performed using the

Kruskal–Wallis test with Tukey–Kramer correction for multigroup comparison.  $*P < 0.05$ . For participant 1, the average reduction of VAS from

before to after the treatments was significant for frequency-invariant stimulation (VAS:  $n = 7$  stimulation sessions, d.f. = 1,  $P = 0.03$ ,  $\chi^2 = 4.52$ )

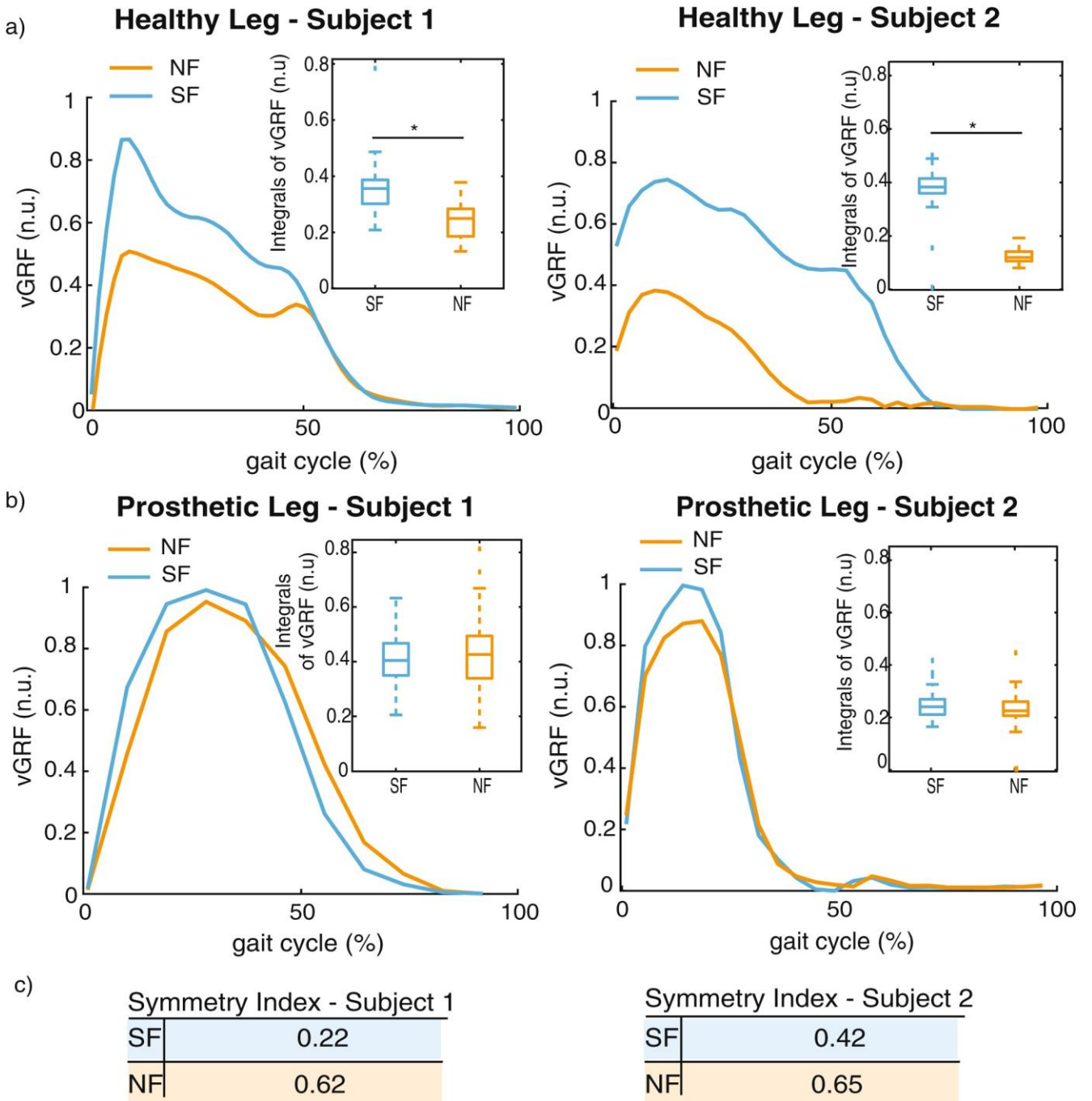
and frequency-variant stimulation ( $n = 7$  stimulation sessions, d.f. = 1,  $P = 0.04$ ,  $\chi^2 = 4.22$ ) as was the case for participant 2 (for frequency-

invariant stimulation,  $n = 10$ , d.f. = 1,  $P = 0.0002$ ,  $\chi^2 = 13.82$ ; for frequency-variant stimulation,  $n = 10$ , d.f. = 1,

$P = 0.009$ ,  $\chi^2 = 6.7$ ). In d,  $P_{\text{frequency-invariant-frequency-variant}} = 0.89$ ,  $P_{\text{frequency-invariant-control}} = 0.0014$ ,  $P_{\text{frequency-variant-control}} = 0.0067$ , d.f. = 2,  $\chi^2_{\text{frequency-invariant-frequency-$

variant} = 8.9,  $\chi^2_{\text{frequency-invariant-control}} = 18.76$ ,  $\chi^2_{\text{frequency-variant-control}} = 17.33$ ; in h,  $P_{\text{frequency-invariant-frequency-variant}} = 0.41$ ,  $P_{\text{frequency-invariant-control}} = 0.000085$ ,  $P_{\text{frequency-variant-$

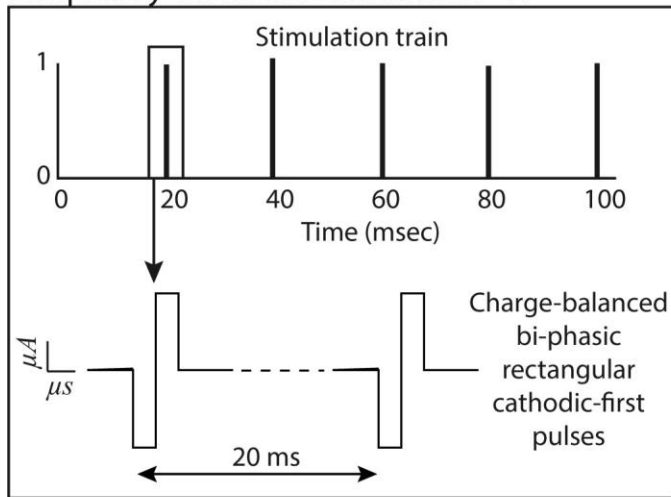
control} = 0.0098, d.f. = 2,  $\chi^2_{\text{frequency-invariant-frequency-variant}} = 13.7$ ,  $\chi^2_{\text{frequency-invariant-control}} = 24.81$ ,  $\chi^2_{\text{frequency-variant-control}} = 20.01$ .



**Extended Data Fig. 4 | Gait analysis during the outdoor sand task.** **a**, Vertical ground reaction force (vGRF) mean value ( $n = 43$  steps) for the healthy leg for participant 1 (left), and vGRF mean value ( $n = 47$  steps) for participant 2 (right). The integrals of vGRF (as function of time; figure insets) are statistically different (ANOVA,  $P < 0.05$ ), showing that higher work is applied on the ground when the feedback (sensory feedback) is provided with regard to the no feedback condition. **b**, vGRF mean value for the prosthetic leg for participants 1 (left) ( $n = 62$  steps) and 2 (right) ( $n = 42$  steps). The integrals of vGRF are not statistically different. n.u., normalized units with respect to the maximum force applied by both feet. In each box plot, the thick horizontal line denotes the median, the lower and upper hinges correspond to the first and third quartiles, the whiskers extend from the hinge to the most extreme value no further than  $1.5 \times$  interquartile range from the hinge and the dots beyond the whiskers are outliers. Statistical evaluations were performed using ANOVA. \* $P < 0.0001$ . Healthy leg, participant 1, d.f. = 1,  $P = 2.89 \times 10^{-8}$ ,  $F = 37.44$ . Prosthetic leg, participant 1: d.f. = 1,  $P = 0.98$ ,  $F = 0$ . Healthy leg, participant 2, d.f. = 1,  $P = 2.87 \times 10^{-37}$ ,  $F = 451.93$ . Prosthetic leg, participant 2, d.f. = 1,  $P = 0.07$ ,  $F = 3.34$ . **c**, Limb Symmetry Index<sup>1</sup> between healthy leg and prosthesis calculated using the mean values of the

integrals of vGRF (a,b). When artificial sensory feedback is provided, the Limb Symmetry Index is closer to 0 than during the no feedback condition. That means that participants are walking more symmetrically, that is, more similarly to how healthy individuals walk.

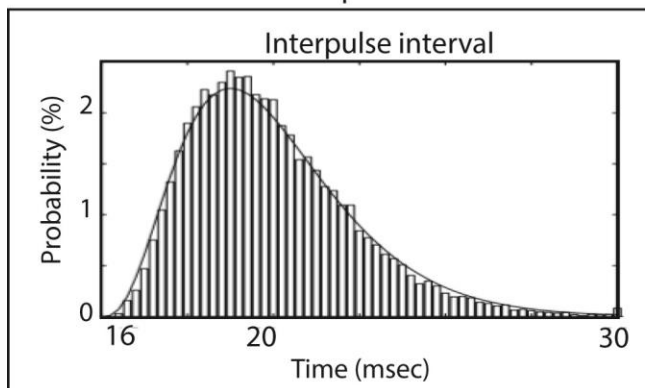
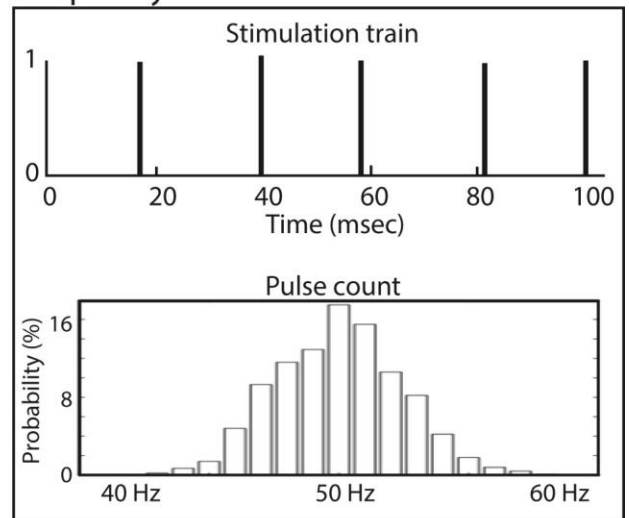
### Frequency-Invariant stimulation - FI



Poissonian noise  
added to 50 Hz



### Frequency-Variant stimulation - FV



**Extended Data Fig. 5 | Pain treatment: frequency-invariant and frequency-variant stimulation.** The stimulation strategies used to treat phantom limb pain are reported. Frequency-invariant stimulation consists of 10-min neural stimulation characterized by constant pulse width, amplitude and frequency (50 Hz). Frequency-variant stimulation is generated using a Poisson noise added at the carrier frequency (50 Hz). The effect is a 10-min pulse train where the inter-pulse interval varies.